Microstructure and Properties of Thermomechanically Strengthened Reinforcement Bars: A Comparative Assessment of Plain-Carbon and Low-Alloy Steel Grades

A. Ray, D. Mukerjee, S.K. Sen, A. Bhattacharya, S.K. Dhua, M.S. Prasad, N. Banerjee, A.M. Popli, and A.K. Sahu

An extensive investigation has been carried out to study structure-property characteristics and corrosion behavior in three varieties of thermomechanically treated (TMT) reinforcement bars (rebars) produced in an integrated steel plant under the Steel Authority of India Limited. Three experimental steel heats—one of plain-carbon and two of low-alloy chemistry—were chosen for the study. Of the two low-alloy heats, one was copper-bearing and the other contained both copper and chromium for improved corrosion resistance. Hot-rolled bars for each specific chemistry were subjected to in-line thermomechanical treatment, where quenching parameters were altered to achieve different yield strength levels.

All the TMT rebars, regardless of chemistry and strength level, exhibited a composite microstructure consisting of ferrite-pearlite at the core and tempered martensite at the rim. Although a tendency toward formation of Widmanstätten ferrite was evident in bars of 500 and 550 MPa yield strength levels, no adverse effect on their strength and ductility was observed. From the standpoint of mechanical properties, the rebars not only conformed to minimum yield strength requirements, but also exhibited high elongation values (21 to 28%) and excellent bendability. Corrosion studies of both TMT and cold-twisted and deformed (CTD) rebars subjected to different laboratory tests indicated that corrosion resistance increased in this order: CTD, plain-carbon TMT, copper-bearing TMT, and copper/chromium-bearing TMT.

Keywords
rebars, tempered martensite, thermomechanical treatment

1. Introduction

THE QUALITY requirements of ribbed steel bars used for concrete reinforcement (rebars) have increased considerably in recent years. Global trends toward weight reduction of steel construction, ease of fabrication, and high dimensional accuracy and stability in handling operations require rebars of high strength (~500 to 550 MPa yield strength) and superior ductility and weldability. The use of high-strength rebars in concrete structures can greatly minimize the consumption of reinforcing steel (Ref 1).

In the past, technologies for achieving high strength in steel bars involved either alloying of steel or work hardening through cold twisting operations. Reinforcement bars that attain high strength through alloying are generally used in the as-rolled condition. These rebars, which are usually of high carbon content (~0.3 to 0.5 wt%), possess restricted weldability, since preheating is necessary and low-heat-input welding often leads to hydrogen embrittlement. On the other hand, work-hardened rebars, which have a lower carbon content (0.06 to 0.15 wt%) and about 1 wt% Mn, have better weldability than alloyed as-rolled rebars. Work-hardened rebars, however, tend to lose their strength upon exposure to temperatures higher than 300 °C, as may often arise during welding or hot-bending operations at the construction site (Ref 2). Although it is possible to produce low-carbon high-strength rebars with good weldability by alloying, the proposition nonetheless is expensive and uneconomical.

Consequently, thermomechanical treatment (TMT) has emerged as a technically attractive route for producing high-strength rebars of lean steel chemistry (Ref 3). The TMT process, in principle, entails in-line water cooling of the hot-rolled bar as it emerges from the last rolling stand. Direct water quenching results in the formation of martensite at the surface layers of the bar while the core remains austenitic. As the bar emerges from the quenching zone, the thermal gradient across the bar section causes heat to flow from the hot austenitic core toward the bar surface. This results in tempering of the surface martensite, and an equalization of surface and core temperatures takes place. For a particular diameter of rebar, the yield strength is dependent on the equalization temperature; lower equalization temperatures result in higher yield strength, and conversely. During subsequent atmospheric cooling of the rolled bar on the cooling bed, the hot austenitic core is gradually transformed to a ferrite-pearlite microstructure. Thermomechanically treated rebars thus develop a composite microstructure: a ductile ferrite-pearlite core and a tough tempered martensite rim. This composite microstructure is primarily responsible for the combination of contradictory metallurgical properties of high strength and ductility.

Experimental trials were carried out at Durgapur Steel Plant under the Steel Authority of India Limited (SAIL) to develop (using the THERMEX process; Hoestemberghe and Klutsch GmbH, Karl-Koch Strasse, D-66787, Wadgassen, Germany)

A. Ray, D. Mukerjee, S.K. Sen, A. Bhattacharya, S.K. Dhua, M.S. Prasad, N. Banerjee, and **A.M. Popli,** Research and Development Centre for Iron and Steel, Steel Authority of India Limited, Ranchi-834002, India, Fax 0651-501327/501489; **A.K. Sahu,** Durgapur Steel Plant, Steel Authority of India Limited, Durgapur-713203, West Bengal, India.

three different varieties of TMT rebars: one of plain-carbon steel (PC-TMT) and two of low-alloy steel chemistries. Of the two low-alloy grades, one heat was copper-bearing (Cu-TMT) and the other was designed to contain copper, chromium, and nickel additions (Cu-Cr-TMT) for improved corrosion resistance. This paper discusses the microstructural and mechanical properties obtained for the various grades of TMT rebars as a function of their steel chemistries and strength levels and compares their corrosion behavior with that of conventional cold-twisted and deformed (CTD) rebars.

2. Experimental

In designing the alloy chemistries, the base compositions (levels of carbon, manganese, silicon, sulfur, and phosphorus) of the three heats were kept similar. One of the low-alloy steel heats contained only copper, while the other contained copper, chromium, and nickel additions. The steels were melted in 220 ton open-hearth furnaces and cast into 8 ton ingots. The chemical analyses of the three heats are shown in Table 1.

The ingots were heated in soaking pits and subsequently rolled in a blooming and billet mill into 100 by 100 mm square billets. The billets were then heated at 1250 to 1300 °C in the reheating furnace and rolled in a merchant mill to 16 and 20 mm diam ribbed bars. The finish rolling temperature of these bars was maintained in the range of 950 to 1000 °C.

The hot-rolled bars were subjected to in-line water quenching after emerging from the last rolling stand, and the quenching parameters (water pressure, volume of water, and number of cooling elements) were altered to achieve different equalization temperatures commensurate with the different yield strength requirements (415, 500, and 550 MPa) of the rebars. The typical operating parameters for achieving different yield strength levels in 16 mm diam TMT ribbed rebars are shown in Table 2.

The quality levels of the various TMT rebars were compared. Their microstructure and mechanical properties were evaluated, and their corrosion characteristics were compared with CTD bars of 415 MPa yield strength.

3. Results and Discussion

3.1 *Steel Chemistry*

The three experimental heats were designed to have a similar base composition (Table 1). The carbon content was kept below 0.2 wt% for weldability considerations, and manganese content was kept in the range of 0.8 to 1.0 wt% for strength contribution. The sulfur and phosphorus contents were restricted to a maximum of 0.04 wt% each.

One of the two low-alloy steel heats was designed to contain only copper (0.30 wt% max), while the other heat had copper (0.30 wt% max), chromium (0.80 wt% max), and nickel (0.30 wt% max) additions to improve corrosion resistance (Ref 4). Although phosphorus is known to improve corrosion resistance, its content was kept low (0.04 wt% max) in the heats because higher levels of carbon and phosphorus individually and synergistically have an adverse effect on toughness and weldability (Ref 4, 5). Composition control in all three experimental heats thus was based on the requirements of steel quality (strength and ductility), weldability, and corrosion resistance. To ensure good weldability, the carbon equivalent (CE), even for the low-alloy steel heats, was kept substantially below 0.55%, which is prescribed as the upper limit for such bars in ASTM A 706/A 706M-90 ("Standard Specification for Low-Alloy Steel Deformed Bars for Concrete Reinforcement").

The CE value is calculated from:

$$CE = \%C + \frac{\%Mn}{6} + \frac{\%Cu}{40} + \frac{\%Ni}{20} + \frac{\%Cr}{10} - \frac{\%Mo}{50} - \frac{\%V}{10} \quad \text{(Eq 1)}$$

The CE values for the PC-TMT, Cu-TMT, and Cu-Cr-TMT compositions (Table 1) were calculated as 0.32, 0.34, and 0.42%, respectively, and thus were significantly lower than the prescribed (CE = 0.55% max) norm.

3.2 *Microstructure*

Transverse sections of the three types of TMT rebars were polished and etched with 2% nital to observe the general mac-

Table 1 Chemical composition of experimental TMT heats

	Chemical composition, wt%								Carbon equivalent,
Steel type	C	Mn	S	P	Si	Cu	Cr	Ni	%
PC-TMT	0.17	0.88	0.038	0.023	0.075	...	...	...	0.32
Cu-TMT	0.18	0.90	0.04	0.035	0.065	0.20	...	...	0.34
Cu-Cr-TMT	0.18	0.82	0.036	0.020	0.070	0.30	0.80	0.30	0.42

Table 2 Typical operating parameters for production of 16 mm diam TMT rebars

Steel grade	Rolling speed, m/s	Finishing temperature, °C	No. of cooling pipes	Water presure, MPa	Water requirement, m^3/h	Equalization temperature, °C
TMT-415	7.95	1000	2	1.4 max	222 max	610
TMT-500	7.95	1000	3	0.8 max	342 max	580
TMT-550	7.95	1000	3	1.2 max	360 max	560

rostructure. A dark peripheral rim of tempered martensite and a gray core corresponding to the ferrite-pearlite interior was observed in all specimens. The area fraction of the tempered martensite rim was found to increase with yield strength (YS) level, the average values being 22.6, 32.2, and 34.8% for bars of 415, 500, and 550 MPa YS levels, respectively. A typical nital-etched macrograph of the transverse polished section of a 20 mm diam TMT rebar of 550 MPa YS grade is shown in Fig. 1. The tempered martensite rim is concentric, indicating uniform quenching of the bar surface in the cooling zone. This uniform rim of tempered martensite results in consistent mechanical properties along the length of the bar.

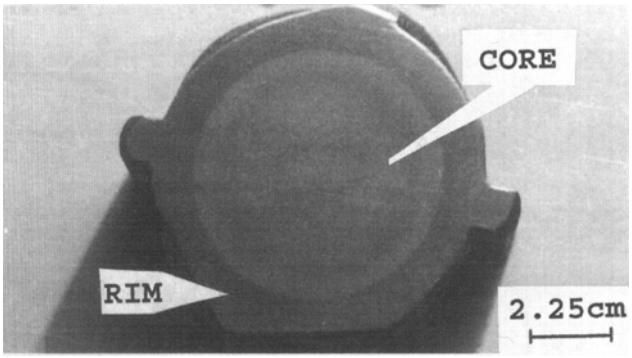

Fig. 1 Nital-etched macrograph of the transverse polished section of a 20 mm diam TMT rebar (550 MPa YS grade), showing a uniform and concentric outer dark etching rim and an inner light gray core

Optical microscopic examinations were carried out in a Neophot-30 model microscope (Carl Zeiss, Jena, Germany) on nital-etched transverse sections of 16 and 20 mm diam TMT and CTD rebars. All the TMT rebars essentially exhibited a composite microstructure comprising a ferrite-pearlitic core and a tempered martensite rim. Typical micrographs of 20 mm diam PC-TMT rebars corresponding to 415, 500, and 550 MPa YS grades are shown in Fig. 2. Similar micrographs for 20 mm diam low-alloy steel Cu-Cr-TMT rebars are depicted in Fig. 3. It is interesting to observe that the core structure consisting of polygonal ferrite and pearlite grains in 415 MPa YS grade bars is gradually transformed into a degenerated appearance at higher yield strength (500 and 550 MPa) levels. As a matter of fact, there is a tendency for the formation of Widmanstätten ferrite, which is markedly visible in the rebars of 500 and 550 MPa YS levels. This is in agreement with the increased quenching rates employed for the production of 500 and 550 MPa YS grade TMT rebars. The incidence of Widmanstätten ferrite is normal for rebars manufactured by the TEMPCORE process

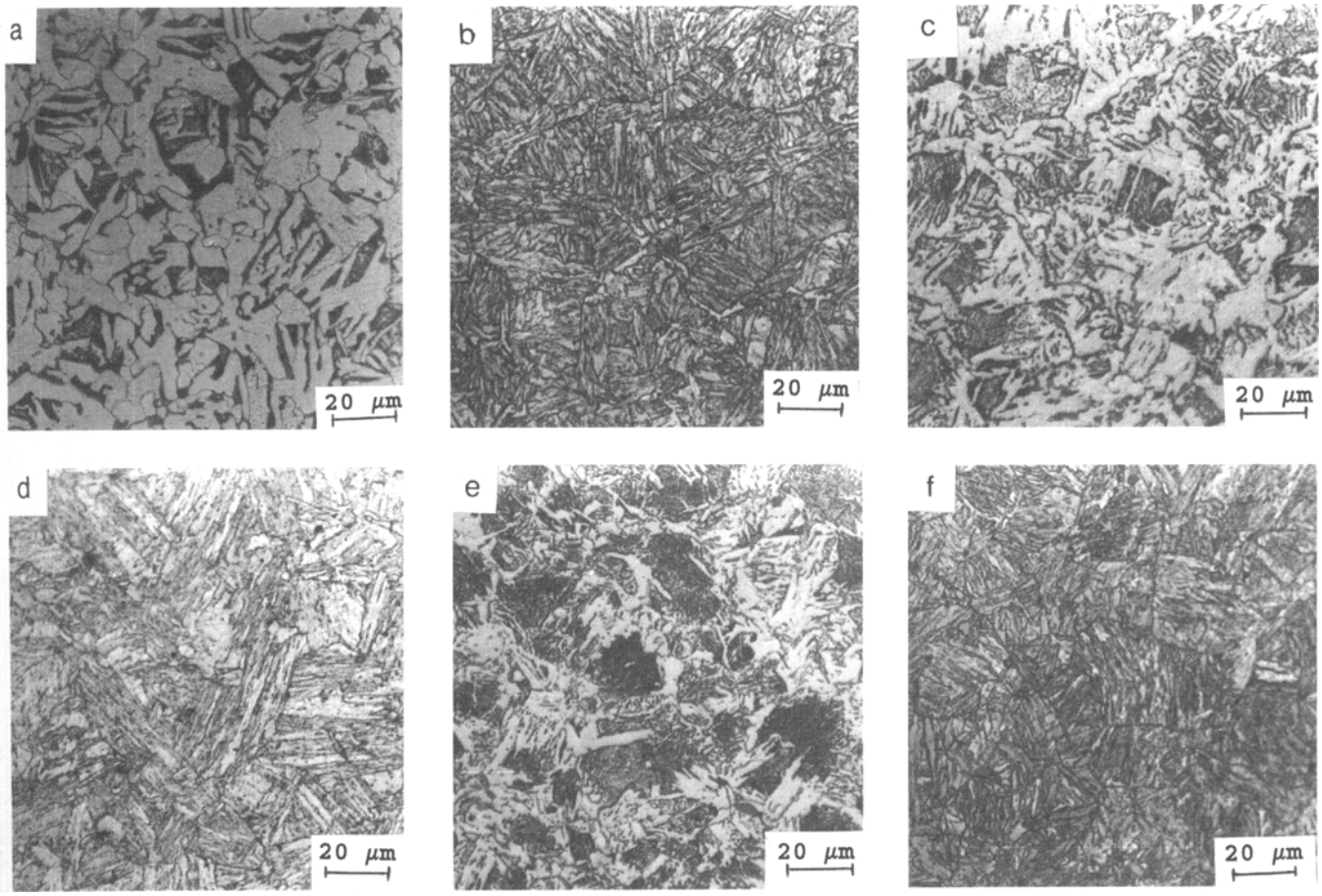

Fig. 2 Microstructure of 20 mm diam plain-carbon TMT rebars showing ferrite-pearlite core and tempered martensite rim. (a) Core, 415 MPa YS grade. (b) Rim, 415 MPa YS grade. (c) Core, 500 MPa YS grade. (d) Rim, 500 MPa YS grade. (e) Core, 550 MPa YS grade. (f) Rim, 550 MPa YS grade

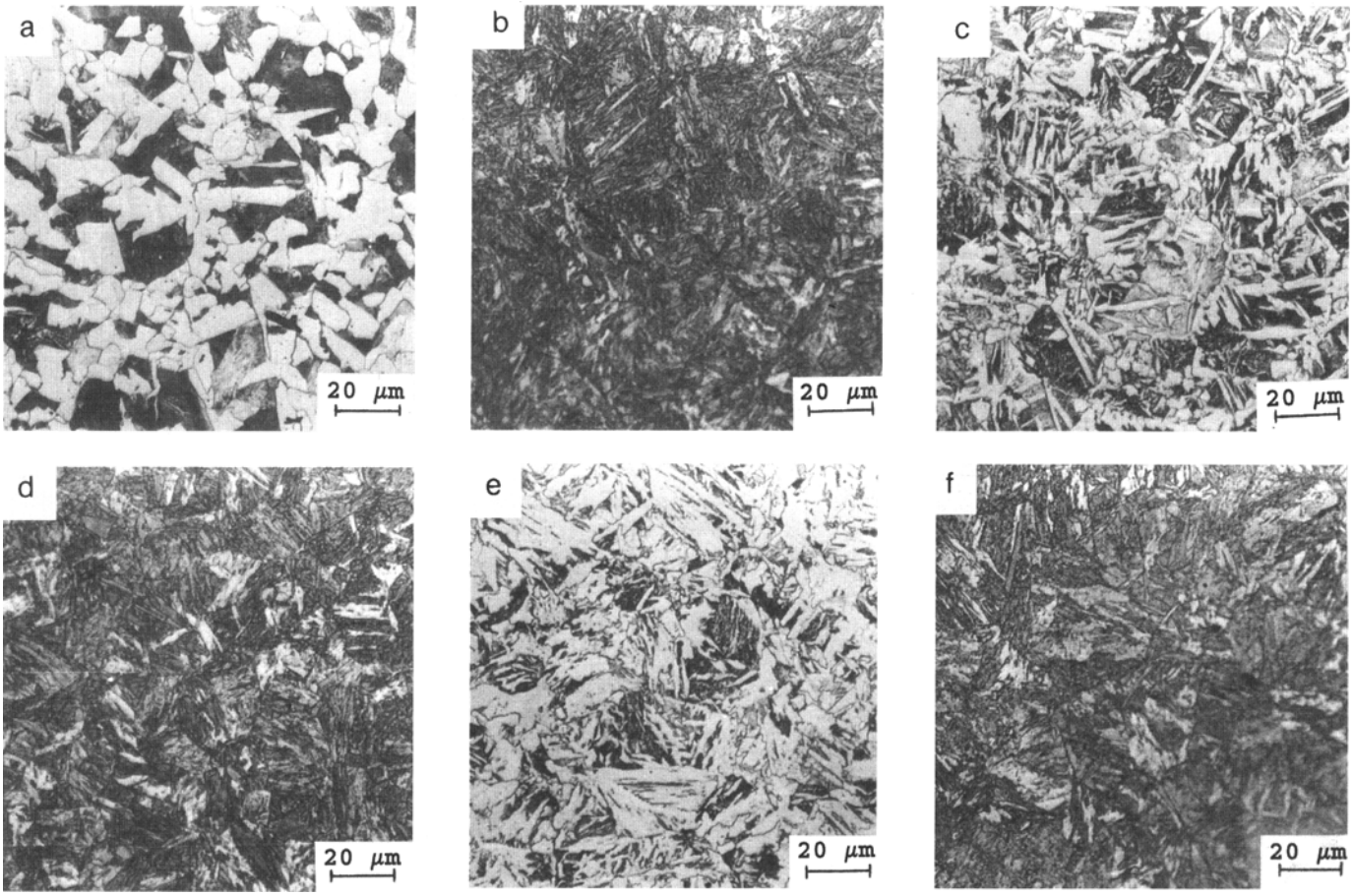

Fig. 3 Microstructure of 20 mm diam Cu-Cr-TMT rebars showing ferrite-pearlite core and tempered martensite rim. (a) Core, 415 MPa YS grade. (b) Rim, 415 MPa YS grade. (c) Core, 500 MPa YS grade. (d) Rim, 500 MPa YS grade. (e) Core, 550 MPa YS grade. (f) Rim, 550 MPa YS grade

Table 3 Mechanical properties of high-strength deformed bars and wires (IS:1786-1985)

Property	Grade		
	Fe 415	Fe 500	Fe 550
Minimum 0.2% proof stress/yield stress, MPa	415	500	550
Minimum percentage of elongation on gage length of $5.65\sqrt{A}$, where A is the cross-sectional area of the testpiece	14.5	12.0	8.0
Minimum tensile strength	10% more than the actual 0.2% proof stress, but not less than 485 MPa	8% more than the actual 0.2% proof stress, but not less than 545 MPa	6% more than the actual 0.2% proof stress, but not less than 585 MPa

(Ref 6). The apparent increase in pearlite content at higher strength levels is presumably attributed to the shifting of the eutectoid point to lower carbon ranges due to faster cooling rates.

Unlike the TMT rebars, the microstructures of 16 and 20 mm diam CTD rebars exhibited normal ferrite-pearlite microstructure at the core as well as at the rim. A typical micrograph of a 20 mm diam CTD bar is shown in Fig. 4.

3.3 *Fractography*

The fracture surfaces of tensile-tested TMT rebars were examined in a JSM-840A model (JEOL Ltd., Tokyo, Japan) scanning electron microscope (SEM). Typical fractographs of 16 mm diam Cu-TMT rebars (500 MPa YS grade) are shown in Fig. 5. The low-magnification photograph in Fig. 5(a) shows a rough-textured core and a relatively smooth rim region. The fractograph of the core region in the same tensile-tested rebar at higher magnification (Fig. 5b) shows a typical dimpled appearance, characteristic of ductile material. The presence of a ductile dimpled core is attributed to the ferrite-pearlite microstructure prevalent there.

3.4 *Tensile Properties*

IS:1786-1985 is the Indian Standard specification for high-strength deformed steel bars and wires for concrete reinforce-

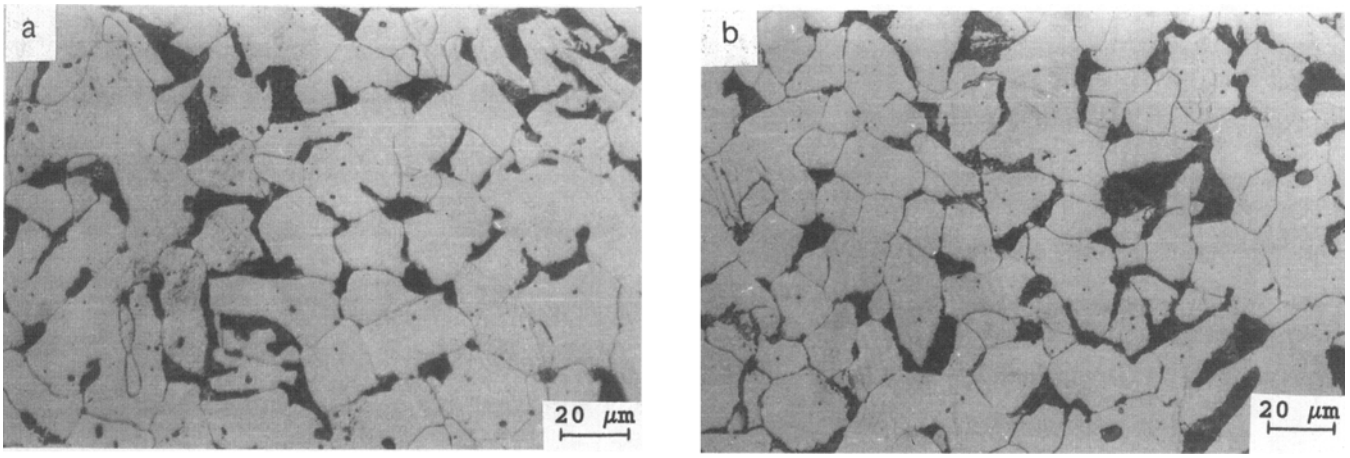

Fig. 4 Typical microstructure of a 20 mm diam CTD rebar showing ferrite and pearlite phases. (a) Core. (b) Periphery

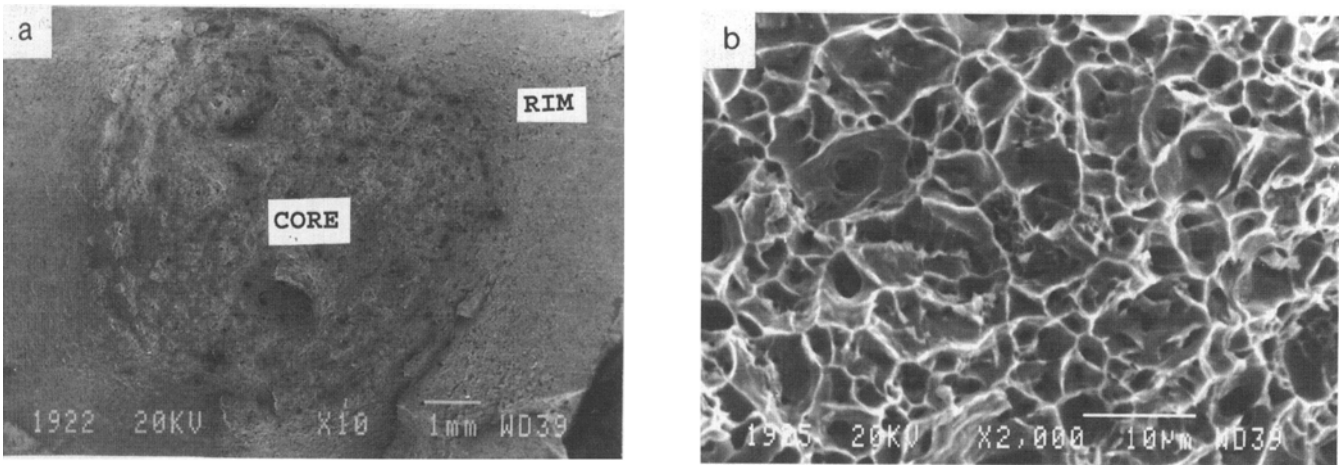

Fig. 5 SEM fractographs of a tensile-tested 16 mm diam Cu-TMT rebar sample. (a) Rough-textured core and relatively smooth rim region. (b) Ductile dimple fracture of core region

ment. The tensile property requirements of rebars according to this specification are shown in Table 3. Tensile tests were carried out on full-section rolled bar specimens; the stress determinations (yield and ultimate tensile strength) were based on the nominal bar area calculated from the weight of a known length of ribbed bar.

The room-temperature tensile properties of ribbed plain-carbon and the two low-alloy steel grades of TMT rebars were evaluated in a 25 ton Instron-1273 model (Instron Ltd., High Wycombe, Bucks, U.K.) dynamic universal testing machine and are shown in Table 4. The values of YS and ultimate tensile strength (UTS) reported in Table 4 represent the average of three samples tested for each variety of rebar. The YS and UTS values obtained for 16 and 20 mm diam TMT rebars conformed to the requirements of IS:1786-1985. The total elongation values (gage length = $5.65\sqrt{A}$, where A is the cross-sectional area of the testpiece) obtained for the three varieties of TMT rebars were found to be greater than 20% for all strength grades. In most cases, the elongation values were greater than 22%. In general, the percentage of elongation for a particular rebar diameter was found to decrease as the designated strength grade (yield strength) of the rebar increased from 415 to 550 MPa. Moreover, in TMT rebars pertaining to a specific chemistry and strength grade, the elongation values, as expected, decreased as the bar diameter increased from 16 mm to 20 mm. The reduction in cross-sectional area of the three types of TMT rebars was also observed to be greater than 50%, indicating high levels of ductility.

As shown, the TMT rebars can achieve high strength levels coupled with high ductility values. This combination can be attributed to the contributions of the tempered martensitic rim and the ferrite-pearlite core, respectively. However, it is important to optimize the quenching parameters such that the area fraction of tempered martensite rim is restricted to around 35% for 550 MPa YS grade bars; greater amounts of tempered martensite inevitably result in higher strength levels at the expense of ductility.

3.5 *Bend Properties*

Bend tests were carried out in accordance with IS:1599-1974 ("Method for Bend Test for Steel Products Other Than Sheet, Strip, Wire and Tube") using mandrels as specified (3*d*, 4*d*, and 5*d* for strength grades corresponding to 415, 500, and 550 MPa YS, where *d* is the nominal diameter of the testpiece

in millimeters, and d is up to 22 mm). The tests were performed on 16 and 20 mm diam PC-TMT, Cu-TMT, and Cu-Cr-TMT rebars of different strength grades. None of the TMT rebars exhibited transverse cracks at the bent regions. In fact, all the rebars exhibited close bend properties without any cracking on the outer side of the bend portion. Figure 6 shows a typical close bend achieved with a 20 mm diam Cu-Cr-TMT rebar of 550 MPa YS grade.

The excellent bendability of all varieties of TMT rebars is attributed to their high ductility (total elongation in the range of 21 to 28%).

3.6 *Corrosion Characteristics*

The corrosion properties of the three types of TMT rebars (500 MPa YS grade) were compared with those of conventional CTD rebars (415 MPa YS grade). Conventional salt-spray and immersion tests as well as accelerated electrochemical corrosion tests employing potentiodynamic measurements were used. The CTD rebars contained 0.24% C, 1.25% Mn, 0.05% S, and 0.05% P (in weight percent).

Corrosion rates in mils per year (1 mil = $^1/_{1000}$ in.) for salt-spray and immersion tests were based on the calculation of weight loss due to corrosion. In the case of potentiodynamic tests, however, the same was determined from corrosion current density (I_{corr}) values based on polarization plots. The corrosion resistance of the rebars was expressed in terms of the corrosion resistance index (CRI), which is a relative measure of the corrosion resistance of a particular grade of steel rebar compared with a reference material. Using CTD rebar as a reference, the CRI value for a specific type of TMT rebar was expressed as CRI_T, the ratio of corrosion rate of CTD rebar in a particular test to the corrosion rate of any specific type of TMT rebar in the same test.

3.6.1 Salt-Spray Test

Salt-spray tests were conducted on the three types of TMT rebars and one type of CTD rebar. The nominal bar diameter se-

Table 4 Tensile properties of experimental TMT rebars

Steel type	Rebar diameter, mm	Designated strength grade, MPa	Yield strength (0.2% proof stress), MPa	Tensile strength, MPa	Elongation, % (gage length = $5.65\sqrt{A}$)
PC-TMT	20	415	493	570	26
		500	530	613	24
		550	565	680	22
Cu-TMT	16	415	474	587	28
		500	529	636	26
		550	566	680	23
	20	415	425	530	23
		500	545	641	22
		550	558	678	21
Cu-Cr-TMT	16	415	444	607	28
		500	543	680	25
		550	576	703	24
	20	415	439	589	27
		500	548	608	25
		550	604	690	22

Table 5 Corrosion characteristics of TMT and CTD rebars

Type of test	Test conditions	Steel type	Strength grade, MPa	Rebar diameter, mm	Corrosion rate		Corrosion resistance index (CRI_T)
					mils/yr	μm/yr	
Salt spray	Solution: 3.5% NaCl Temperature: 28 ± 2 °C Duration: 720 h	CTD	415	20	21.24	539.50	...
		PC-TMT	500	20	19.60	497.84	1.08
		Cu-TMT	500	20	18.75	476.25	1.13
		Cu-Cr-TMT	500	20	15.20	386.08	1.40
Immersion	Solution: 3.5% NaCl Temperature: 28 ± 2 °C Duration: 720 h	CTD	415	20	22.47	570.74	...
		PC-TMT	500	20	20.13	511.30	1.12
		Cu-TMT	500	20	19.36	491.74	1.16
		Cu-Cr-TMT	500	20	16.34	415.04	1.38
Potentiodynamic	Solution: 3.5% NaCl Temperature: 28 ± 2 °C Scan speed: 1 mV/s	CTD	415	16	36.27	921.26	...
		Cu-TMT	500	16	27.70	703.58	1.31
		Cu-Cr-TMT	500	16	23.86	606.04	1.52

lected for the test was 20 mm, and the test was carried out in accordance with ASTM B 117-90 specifications. Experiments were conducted in a salt-spray chamber using a nominal sample length of 10 cm at an ambient temperature of 28 ± 2 °C. Both transverse cut ends of each sample were masked with lacquer so that only the ribbed longitudinal surfaces were exposed to the salt fog environment.

The salt solution was prepared by dissolving analytical-grade NaCl in distilled water to obtain 3.5% salt concentration. This solution was then poured inside the spray chamber and injected in the form of salt fog by the action of compressed air through a specially designed nozzle. The samples were carefully cleaned and weighed prior to masking of the cut ends and insertion in the chamber.

After exposure to the salt fog atmosphere for 720 h, the samples were removed from the chamber, lightly scrubbed with a metal brush under running water to remove corrosion products, and washed in soap solution to remove dirt and other greasy substances. The samples were then cleaned in acetone to remove the mask and dried. They were again weighed to determine the weight loss due to corrosion. From the weight loss data, corrosion rates were calculated.

Table 5 shows the corrosion rates of different types of ribbed bars during salt-spray testing. The corrosion rates were based on average values taken from three samples for each type of rebar. From these data, CRI_T values for the TMT rebars were calculated. The results indicate that CTD rebars have the highest corrosion rate, followed by PC-TMT, Cu-TMT, and Cu-Cr-TMT rebars. Although corrosion is known to be accentuated at higher strength levels, all varieties of 500 MPa YS grade TMT rebars were found to exhibit superior corrosion resistance compared to the lower-strength (415 MPa YS) CTD rebars.

The difference in corrosion behavior essentially lies in the fact that unlike CTD rebars, which are twisted, TMT rebars are devoid of any torsional stresses on the surface. It is well known that cold working of carbon steel tends to increase corrosion rates (Ref 7). The absence of torsional stresses and the lower carbon content (0.17 wt%) in PC-TMT rebars compared to higher carbon (0.24 wt%) in CTD rebars facilitate better corrosion resistance in the former.

Among the different varieties of TMT rebars, it is clearly evident that corrosion rate is influenced by chemical composition. The TMT rebars containing 0.30 wt% Cu and 0.80 wt% Cr showed the lowest corrosion rate in the NaCl environment. This is expected, because both copper and chromium are known to improve corrosion resistance (Ref 8). The Cu-TMT rebars also showed corrosion resistance marginally better than PC-TMT rebars by virtue of the beneficial effect of copper.

From the CRI_T values for the salt-spray test given in Table 5, it is evident that TMT rebars are more corrosion resistant than conventional CTD rebars. In fact, PC-TMT, Cu-TMT, and Cu-Cr-TMT rebars were found to be 1.08, 1.13, and 1.40 times more corrosion resistant, respectively, than the CTD rebars.

3.6.2 Immersion Test

Immersion testing also was carried out using CTD rebar and the three types of TMT rebars, all 20 mm in diameter. The tests were conducted in accordance with ASTM G 3172-90. The rebar test samples had a nominal length of 10 cm, and their transverse cut ends were masked with lacquer so that only the longitudinal ribbed surfaces were exposed to the solution during immersion. The samples were cleaned, dried, and weighed before masking and then fully immersed in freshly prepared 3.5% NaCl solution. The volume of the test solution was sufficiently large to avoid any appreciable change in its corrosivity during the tests.

Testing was conducted at an ambient temperature of 28 ± 2 °C. The samples were immersed in the test solution for 720 h. After exposure, they were removed from the solution, cleaned, and weighed. The difference between the initial and final weights was used to calculate the corrosion rate. Three samples were tested for each type of rebar, and the average corrosion rates are shown in Table 5.

The immersion test results given in Table 5 show that corrosion behavior followed the same trend as that experienced during salt-spray testing. The corrosion rates in ascending order are: Cu-Cr-TMT, Cu-TMT, PC-TMT, and CTD rebars. The Cu-Cr-TMT rebars exhibited the best corrosion resistance, which can be attributed to the beneficial effect of both copper and chromium in inhibiting corrosion. The CRI_T values of the TMT rebars signified corrosion resistance 1.12 to 1.38 times higher than that of conventional CTD rebar. As in the salt-spray experiments, the CRI_T value markedly increased for Cu-Cr-

Fig. 6 Photograph of close bend obtained in a 20 mm diam Cu-Cr-TMT rebar (550 MPa YS grade) showing no manifestation of surface cracks

TMT rebars (1.38) in comparison to Cu-TMT rebars (1.16). This indicates that Cu-Cr-TMT rebars possess superior corrosion resistance compared to Cu-TMT rebars under identical test conditions. The Cu-TMT rebars displayed a slightly better CRI_T value compared to PC-TMT rebars. As expected, the CTD rebar exhibited the lowest corrosion resistance (see section 3.6.1).

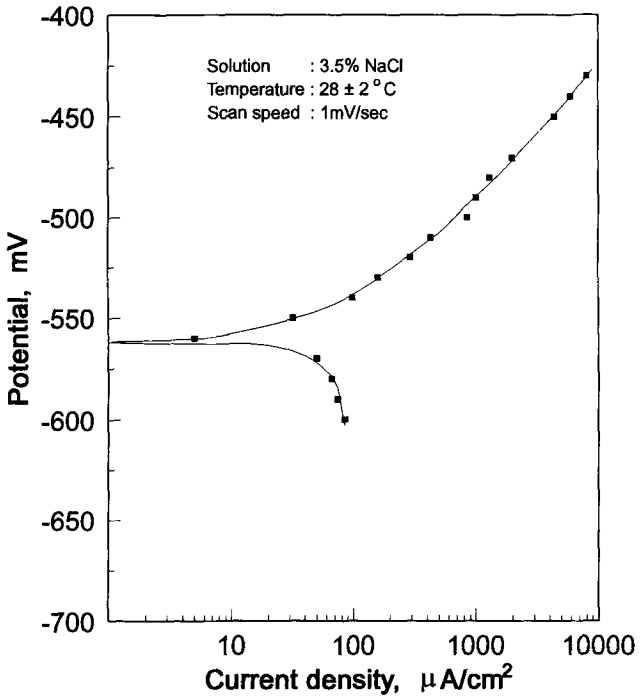

Fig. 7 Polarization plot of a 16 mm diam Cu-Cr-TMT rebar (500 MPa YS grade)

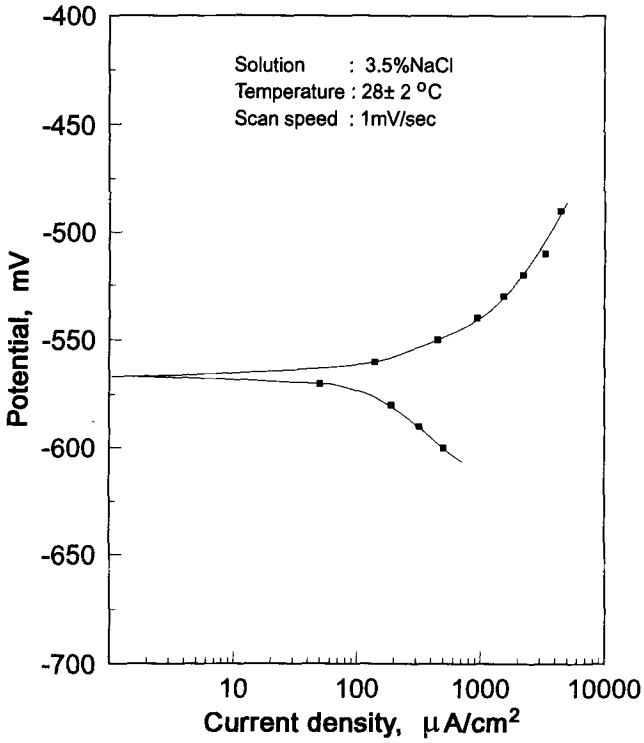

Fig. 8 Polarization plot of a 16 mm diam CTD rebar (415 MPa YS grade)

3.6.3 Potentiodynamic Test

The electrochemical corrosion behavior of the various rebars was studied by the accelerated potentiodynamic corrosion test, in which the surface current density is scanned over a potential range. Conducted on 16 mm diam Cu-TMT, Cu-Cr-TMT, and CTD rebars in accordance with ASTM G 5-87, the potentiodynamic tests were carried out in 3.5% NaCl solution at an ambient temperature of 28 ± 2 °C. The experiments were undertaken in an AMEL model 549 potentiostat (Apparecchiature Di Misura Elettroniche, Via Bolzano, Milan, Italy). Samples 1 cm long were cut, and the two cut ends were masked with lacquer to expose only the ribbed surface during measurements. One sample for each of the three types of rebars was tested.

During the test, potential was scanned from the cathodic to the anodic region at a rate of 1 mV/s to obtain polarization plots. Typical polarization plots obtained for Cu-Cr-TMT and CTD rebars are shown in Fig. 7 and 8, respectively. Values of I_{corr} were obtained from the plots in the standard manner, and the corrosion rate was determined from the following empirical formula (Ref 9):

$$\text{Corrosion rate (mils/year)} = \frac{0.1288 \times I_{corr} \times W}{d} \qquad \text{(Eq 2)}$$

where I_{corr} is the corrosion current density in $\mu A/cm^2$, W is the equivalent weight of steel (27.925 g), and d is the density of steel (7.85 g/cm^3).

The corrosion rates exhibited by the different types of rebars in this test (Table 5) follow the same trend as was exhibited in the salt-spray and immersion tests. The corrosion rate was found to be highest (36.27 mils/year) for the CTD rebar and lowest (23.86 mils/year) for the Cu-Cr-TMT rebar. The Cu-TMT rebar exhibited a corrosion rate of 27.70 mils/year. The corrosion behavior of the CTD and TMT rebars thus seems to have been influenced by two factors: surface torsional stresses and steel chemistry (see section 3.6.1).

The CRI_T values obtained in the potentiodynamic tests elucidate the vastly superior corrosion resistance of TMT rebars with respect to CTD rebars. The Cu-TMT and Cu-Cr-TMT rebars were found to be, respectively, 1.31 and 1.52 times more corrosion resistant than conventional CTD rebar.

3.6.4 Corrosion Behavior: TMT Versus CTD Rebars

The results of the three different types of corrosion tests unambiguously demonstrate the superior corrosion characteristics of TMT rebars compared to CTD rebars. The corrosion rates of CTD rebars were found to be 8.4 to 52% higher than TMT rebars, depending on the nature of the test and the type of TMT rebar.

Among the different varieties of TMT rebars tested, the copper/chromium-bearing bars exhibited superior corrosion resistance and the lowest corrosion rates. The CTD rebars, despite their lower YS level (415 MPa), displayed corrosion rates sig-

nificantly higher than the higher YS grade (500 MPa) Cu-Cr-TMT bars—to the extent of 37.5 to 52% in various tests. The Cu-TMT rebars exhibited slightly better corrosion resistance than the PC-TMT rebars, but were inferior to the Cu-Cr-TMT rebars.

In general, the corrosion rates experienced in the potentiodynamic test were higher than in the salt-spray or immersion tests. In electrochemical tests involving potentiodynamic measurements, accelerated corrosion is induced by making the rebar initially cathodic and then anodic by imposing an external potential. For Cu-Cr-TMT rebars, the surface becomes covered with a protective layer of chromium oxide film due to preferential oxidation of chromium by the nascent oxygen evolved at the anode. In contrast, the CTD rebar surface does not become covered with a protective film and therefore exhibits a higher corrosion rate. The Cu-TMT rebars perform better than CTD rebars by virtue of the ability of copper to lower the activity of iron at the surface and because the rust on copper-bearing steels is sufficiently compact to eventually retard the rate of corrosion (Ref 7).

It is interesting to observe that lower YS grade CTD rebars exhibit higher corrosion rates than untwisted TMT rebars of higher YS levels. Higher carbon and manganese contents in CTD rebars induce greater heterogeneity in the microstructure; the resulting increased pearlite volume fraction enhances the tendency for electrochemical cell formation. Further, the presence of surface torsional stresses on CTD rebars induces a higher corrosion rate. Besides, low-alloy TMT rebars containing either copper or copper, chromium, and nickel have better corrosion resistance by virtue of their intrinsic nature.

4. Conclusions

Thermomechanically treated rebars of different yield strength grades (415, 500, and 550 MPa) were produced through proper control of quenching parameters (water pressure, water volume, and number of cooling elements) in plain-carbon and low-alloy steel grades containing either copper or copper, chromium, and nickel additions. These rebars, regardless of chemistry and strength grade, exhibited a composite microstructure comprising a ferrite-pearlite core and a tempered martensite rim. The tempered martensite rim was found to be concentric and uniform, its area fraction increasing from 22.6% in 415 MPa YS grade rebars to 34.8% in 550 MPa YS grade rebars. The core structure in 415 MPa YS grade rebars consisted of polygonal ferrite and pearlite. However, at increased strength levels (500 and 550 MPa YS), there was a tendency toward formation of Widmanstätten ferrite with no adverse effect on mechanical properties.

All the TMT rebars exhibited high ductility at all yield strength levels up to 550 MPa. With respect to YS, UTS, percentage of elongation, and bendability, these rebars were not only in conformity, but also displayed superior properties than those required under IS:1786-1985. In fact, these rebars could be close bent without exhibiting cracks, and the total elongation values attained (21 to 28%) far exceed the specified minimum requirements. The attainment of high strength coupled with high ductility values is attributed to the contributions made by the tempered martensite rim and the ferrite-pearlite core. However, it is important to restrict the overall area fraction of the tempered martensite rim within 35%, in the case of 550 MPa YS grade rebars, for ductility considerations.

Laboratory corrosion tests (salt spray, immersion, and potentiodynamic) clearly indicated that the corrosion rates increase in this order: Cu-Cr-TMT, Cu-TMT, PC-TMT, and CTD rebars. The low-alloy TMT grades (copper-bearing and copper/chromium-bearing) were found to be 1.13 to 1.52 times more corrosion resistant than CTD rebars, depending on the type of test, whereas the PC-TMT rebars were 1.08 to 1.12 times more corrosion resistant than CTD rebars.

The CTD rebar exhibited the poorest corrosion behavior due to its higher carbon and manganese contents, as well as the presence of surface torsional stresses. Among the TMT rebars, the Cu-Cr-TMT type had the best corrosion characteristics in view of the roles of copper, chromium, and nickel in inhibiting corrosion.

Acknowledgments

The authors are grateful to the managements of the R&D Centre and the Durgapur Steel Plant of SAIL for their encouragement and support. Thanks are due to the technical personnel of the Mechanical Testing and Metallography Laboratories of the R&D Centre and to Mr. R. Roy Choudhury and B. Khalkho for typing the manuscript.

References

1. Y.T. Khudik, A.V. Ivchenko, O.A. Chaikovskii, S.A. Madtyan, M.I. Kostyuchenko, and I.N. Surikov, Thermomechanically Strengthened 25G2S Reinforcing Steel of Strength Class At-IVS, *Steel USSR,* Vol 18 (No. 6), 1988, p 272-277
2. K. Frommann and C.M. Vlad, Mechanical and Technological Properties of TEMPRIMAR Weldable High Strength Rebars, *27th Mechanical Working and Steel Processing Conf. Proc.,* Vol 23, Iron and Steel Society, 1986, p 901-907
3. S.A. Madatyan, Main Trends in Development of Production and Use of Steel Reinforcing Bars, *Steel USSR,* Vol 21 (No. 7), 1991, p 322-325
4. T. Zaizen, T. Watanabe, K. Okamato, K. Kanaya, M. Sato, T. Haze, and Y. Ohno, Low C-Cu-P Type Superior Atmospheric Corrosion Resistant Steel for Welded Structures, *Nippon Steel Tech. Rep.,* No. 22, Dec 1983, p 61-73
5. D.T. Llewellyn, Low-Carbon Structural Steels, *Steels: Metallurgy and Applications,* Butterworth Heinemann, 1992, p 64-119
6. C.M. Vlad, A Comparison between the TEMPRIMAR and TEMPCORE Processes for Production of High Strength Rebars, *27th Mechanical Working and Steel Processing Conf. Proc.,* Vol 23, Iron and Steel Society, 1986, p 909-912
7. S.L. Chawla and R.K. Gupta, Factors Influencing Corrosion and Its Forms, *Material Selection for Corrosion Control,* ASM International, 1993, p 29-63
8. W.K. Boyd and F.W. Fink, "Corrosion of Metals in the Atmosphere," MCIC Report No. 74-23, Battelle Columbus Laboratories, Aug 1974, p 1-77
9. S.W. Dean, Jr., Electrochemical Methods of Corrosion Testing, *Electrochemical Techniques for Corrosion,* R. Baboian, Ed., National Association of Corrosion Engineers, 1978, p 52-60